Research Article | Vol. 25, No. 3 | 6 Feb 2017 | OPTICS EXPRESS 1710

Optics EXPRESS

Modelling end-pumped passively Q-switched Nd-doped crystal lasers: manifestation by a Nd:YVO_4/Cr^{4+}:YAG system with a concave-convex resonator

P. H. TUAN, C. C. CHANG, F. L. CHANG, C. Y. LEE, C. L. SUNG, C. Y. CHO, Y. F. CHEN, AND K. W. SU*

Department of Electrophysics, National Chiao Tung University, 1001, Ta-Hsueh Rd., Hsinchu 30010, Taiwan

sukuanwei@mail.nctu.edu.tw

Abstract: A theoretical model for the passively Q-switched (PQS) operation which includes the spatial overlapping between the pump and lasing modes under the thermal lensing effect is developed to give a transcendental equation that can directly determine the critical parameters such as pulse energy, pulse repetition rate, and pulse width for the PQS performance. More importantly, an analytical function which gives the approximate solution for the transcendental equation as well as a specific critical criterion for good PQS operation are derived for practical analyses and design. A Nd:YVO_4/Cr^{4+}:YAG system with a concave-convex resonator which can achieve fairly stable PQS pulse trains even at a high pump level is further exploited to manifest the proposed spatially dependent model. The good agreement between the experimental results and the theoretical predictions is verified to show the feasibility of the proposed model for designing high-power PQS lasers with high accuracy.

OCIS codes: (140.3430) Laser theory; (140.3540) Lasers, Q-switched; (140.3538) Lasers, pulsed.

References and links

1. J. E. Nettleton, B. W. Schilling, D. N. Barr, and J. S. Lei, "Monoblock laser for a low-cost, eyesafe, microlaser range finder," Appl. Opt. **39**(15), 2428–2432 (2000).
2. S. M. Hannon and J. A. Thomson, "Aircraft wake vortex detection and measurement with pulsed solid-state coherent laser radar," J. Mod. Opt. **41**(11), 2175–2196 (1994).
3. I. N. Smalikho and S. Rahm, "Lidar investigation of the effect of wind and atmospheric turbulence on aircraft wake vortices," Opt. Atmosf. Okeana **22**(2), 1160–1169 (2009).
4. M. Malinauskas, A. Žukauskas, S. Hasegawa, Y. Hayasaki, V. Mizeikis, R. Buividas, and S. Juodkazis, "Ultrafast laser processing of materials: from science to industry," Light Sci. Appl. **5**(8), e16133 (2016).
5. N. Pavel, M. Tsunekane, and T. Taira, "Composite, all-ceramics, high-peak power Nd:YAG/Cr^{4+}:YAG monolithic micro-laser with multiple-beam output for engine ignition," Opt. Express **19**(10), 9378–9384 (2011).
6. Y. J. Huang, Y. P. Huang, P. Y. Chiang, H. C. Liang, K. W. Su, and Y. F. Chen, "High-power passively Q-switched Nd:YVO_4 UV laser at 355 nm," Appl. Phys. B **106**(4), 893–898 (2012).
7. A. E. Siegman, *Lasers* (University Science Books, 1986), Chap. 26.
8. A. Agnesi and S. Dell'Acqua, "High-peak-power diode-pumped passively Q-switched Nd:YVO_4 laser," Appl. Phys. B **76**(4), 351–354 (2003).
9. M. Arvidsson, "Far-field timing effects with passively Q-switched lasers," Opt. Lett. **26**(4), 196–198 (2001).
10. A. Ishaaya, N. Davidson, and A. Friesem, "Very high-order pure Laguerre-Gaussian mode selection in a passive Q-switched Nd:YAG laser," Opt. Express **13**(13), 4952–4962 (2005).
11. S. Forget, F. Druon, F. Balembois, P. Georges, N. Landru, J.-P. Fève, J. Lin, and Z. Weng, "Passively Q-switched diode-pumped Cr^{4+}:YAG/Nd:$GdVO_4$ monolithic microchip laser," Opt. Commun. **259**(2), 816–819 (2006).
12. G. M. Thomas and M. J. Damzen, "Passively Q-switched Nd:YVO_4 laser with greater than 11 W average power," Opt. Express **19**(5), 4577–4582 (2011).
13. X. Li, G. Li, S. Zhao, K. Yang, T. Li, G. Zhang, K. Cheng, and X. Wang, "Passively Q-switched diode-pumped Cr^{4+}:YAG/Nd^{3+}:$GdVO_4$ monolithic microchip laser," Opt. Laser Technol. **44**(4), 929–934 (2012).
14. A. Szabo and R. A. Stein, "Theory of laser giant pulsing by a saturable absorber," J. Appl. Phys. **36**(5), 1562–1566 (1965).

#283222 http://dx.doi.org/10.1364/OE.25.001710
Journal © 2017 Received 19 Dec 2016; revised 13 Jan 2017; accepted 16 Jan 2017; published 23 Jan 2017

Optics EXPRESS

15. J. J. Degnan, "Optimization of passively Q-switched lasers," IEEE J. Quantum Electron. **31**(11), 1890–1901 (1995).
16. G. Xiao and M. Bass, "A generalized model Q-switched lasers including excited state absorption in the saturable absorber," IEEE J. Quantum Electron. **33**(1), 41–44 (1997).
17. X. Zhang, S. Zhao, Q. Wang, Q. Zhang, L. Sun, and S. Zhang, "Optimization of Cr^{4+}-doped saturable-absorber Q-switched lasers," IEEE J. Quantum Electron. **33**(12), 2286–2294 (1997).
18. Y. F. Chen, Y. P. Lan, and H. L. Chang, "Analytical model for design criteria of passively Q-switched lasers," IEEE J. Quantum Electron. **37**(3), 462–468 (2001).
19. X. Zhang, S. Zhao, Q. Wang, B. Ozygus, and H. Weber, "Modeling of passively Q-switched lasers," J. Opt. Soc. Am. B **17**(7), 1166–1175 (2000).
20. N. Pavel, J. Saikawa, S. Kurimura, and T. Taira, "High average power diode end-pumped composite Nd:YAG laser passively Q-switched by Cr^{4+}:YAG saturable absorber," Jpn. J. Appl. Phys. **40**(3A), 1253–1259 (2001).
21. Y. F. Chen, T. M. Huang, C. F. Kao, C. L. Wang, and S. C. Wang, "Optimization in scaling fiber-coupled laser-diode end-pumped lasers to higher power: influence of thermal effect," IEEE J. Quantum Electron. **33**(8), 1424–1429 (1997).
22. W. A. Clarkson, R. Koch, and D. C. Hanna, "Room-temperature diode-bar-pumped Nd:YAG laser at 946 nm," Opt. Lett. **21**(10), 737–739 (1996).
23. C. Y. Cho, Y. P. Huang, Y. J. Huang, Y. C. Chen, K. W. Su, and Y. F. Chen, "Compact high-pulse-energy passively Q-switched Nd:YLF laser with an ultra-low-magnification unstable resonator: application for efficient optical parametric oscillator," Opt. Express **21**(2), 1489–1495 (2013).
24. Y. F. Chen, C. F. Kao, T. M. Huang, C. L. Wang, and S. C. Wang, "Influence of thermal effect on output power optimization in fiber-coupled laser-diode end-pumped lasers," IEEE J. Sel. Top. Quantum Electron. **3**(1), 29–34 (1997).
25. Y. T. Chang, Y. P. Huang, K. W. Su, and Y. F. Chen, "Comparison of thermal lensing effects between single-end and double-end diffusion-bonded Nd:YVO4 crystals for 4F 3/2-->4I 11/2 and 4F 3/2-->4I 13/2 transitions," Opt. Express **16**(25), 21155–21160 (2008).
26. R. B. Chesler and D. Maydan, "Convex-concave resonators for TEM_{00} operation of solid-state ion lasers," J. Appl. Phys. **43**(5), 2254–2257 (1972).
27. P. H. Tuan, C. C. Chang, C. Y. Lee, C. Y. Cho, H. C. Liang, and Y. F. Chen, "Exploiting concave-convex linear resonators to design end-pumped solid-state lasers with flexible cavity lengths: Application for exploring the self-mode-locked operation," Opt. Express **24**(23), 26024–26034 (2016).
28. Y. F. Chen, T. M. Huang, C. F. Kao, C. L. Wang, and S. C. Wang, "Generation of Hermite-Gaussian modes in fiber-coupled laser-diode end-pumped lasers," IEEE J. Quantum Electron. **33**(6), 1025–1031 (1997).

1. Introduction

Passively Q-switched (PQS) solid-state lasers with the advantages of compactness, high reliability, and low cost have been extensively developed to offer high-peak-power and high-pulse-energy light sources for various applications such as range finders [1], remote sensing [2], lidars [3], material processing [4], laser ignition [5], and nonlinear optics [6]. Unlike actively Q-switching (AQS) with an external electronic controller, the performance of passively Q-switching is dominated by the saturation mechanism which is closely related to the initial transmission and the irradiated photon density of the absorber [7]. As a consequence, it is of great importance to control the intracavity mode size to effectively bleach the saturable absorber for building up a stable giant pulse [6,8]. To avoid pulse instability caused by the parasitic effect due to the asynchronous bleach of absorber with respect to different high-order transverse modes [9, 10], the end pumping scheme is frequently adopted for achieving good TEM_{00} mode operation in PQS lasers. However, the serious thermal lensing effect of the end-pumped crystal lasers significantly influences the stability and oscillation mode size of the cavity, leading the pulse repetition rate, pulse energy, and pulse width to present behavior that is greatly different from the theoretical predictions at higher pump level [11–13]. So far a theoretical model with the consideration of varying mode size due to the thermal lensing effect is highly desirable for practically designing and accurately analyzing high-power PQS lasers.

The essential elements to model the PQS operation are the coupled rate equations first derived by Szabo and Stein [14]. Following the seminal work, several generalized models to optimize the PQS performance have been successively proposed [15–18]. Degnan introduced his elegant approach to obtain closed form solutions for key laser parameters such as output energy and pulsewidth and to determine the optimum design criterion in terms of the gain factor [15]. Modifying Degnan's method, Xiao *et al* [16] and Zhang *et al* [17] included the

Optics EXPRESS

excited state absorption (ESA) of the saturable absorber into the rate equations for more accurate analyses. Chen *et al.* further considered the influence of intracavity focusing into the modified model and derived an analytical expression to determine optimum initial transmission of absorber and optimum reflectivity of output coupler for a practical design [18]. However, most of these treatments are based on the plane-wave approximation in which the pumping profile, the intracavity photon intensity, and the bleaching of absorber are assumed to be spatially uniform. There are only few investigations reported to consider the spatial dependences of the intensity of intracavity photon, inversion population of gain medium, and the ground-state population of absorber into the PQS models [19, 20]. Since the spatial variation of cavity mode has been confirmed to be important for the output efficiency of end-pumped lasers [21], an analytical model which integrates the present treatments for PQS operation with the modification of mode-size dependence on the thermal lensing is worthwhile to be developed.

In this work, we start from the coupled rate equations given in [18] to explicitly derive a transcendental equation whose solution can straightforwardly determine the critical characteristics of pulse energy, pulse repetition rate, and pulse width for the PQS lasers. With the numerical fitting, the solution of the transcendental equation is found that can be approximated by an analytical function that is greatly useful for practical design and analyses. More importantly, it is confirmed that the approximated solution is not only feasible for PQS operation but also valid for AQS lasers under the rapid Q-switching condition. For generalizing the theoretical results into a spatially dependent model, we further consider the spatial overlapping between the pump and lasing modes influenced by the thermal lensing into the analysis. The modified model reveals that there are significant differences of the PQS performance between the theoretical predictions with and without the spatial dependence. In order to prove the validity of the modified theory for analyzing PQS lasers in a real case, an end-pumped Nd:YVO_4/Cr^{4+}:YAG system with a concave-convex resonator is utilized for manifestation. Compared with the PQS performance of a conventional concave-plano cavity, the concave-convex resonator with large mode volume [22, 23] is found that can meet the second threshold criterion and achieve energy scale-up very easily. The experimental pulse trains with little time jitters and small amplitude fluctuations even under a high-power pump show that the concave-convex resonator is advantageous for designing PQS lasers with a stable output performance. Finally, it is confirmed that all experimental pulse energy, pulse repetition rate, and pulse width can be described in perfect consistency by using the modified PQS model. The good agreement between the experimental results and theoretical predictions sheds light on using the developed spatially dependent model to design and analyze high-power PQS practically.

2. Modified model for PQS operation under the influence of thermal lensing

At first we give a thorough review of the approach proposed in [18] to derive a concise expression for describing the performance of the PQS lasers. The coupled rate equations for a four-level system in the PQS operation with the effects of ESA and intracavity focusing are given by

$$\frac{d\phi}{dt}=\frac{\phi}{t_r}\left[2\sigma n l_g-2\sigma_{gs}n_{gs}l_s-2\sigma_{es}n_{es}l_s-\left(\ln\left(\frac{1}{R}\right)+L\right)\right], \tag{1}$$

$$\frac{dn}{dt}=-c\sigma n\phi, \tag{2}$$

$$\frac{dn_{gs}}{dt}=-\frac{A}{A_s}c\sigma_{gs}n_{gs}\phi, \tag{3}$$

Optics EXPRESS

where ϕ is the intracavity photon density; n is the inversion population density of the gain medium; l_g is the length of the gain medium; l_s is the length of the saturable absorber; A/A_s is the ratio between the effective mode area at the gain medium and at the saturable absorber; n_{gs}, n_{es}, and n_{so} are the ground, excited states, and total population densities of the absorber; σ_{gs}, and σ_{es} are the GSA and ESA cross sections of the absorber, respectively; R is the reflectivity of the output coupler (OC); L is the round-trip optical loss; $t_r = 2l_{cav}/c$ is the round-trip time of light with respect to the cavity length l_{cav}, and c is the light speed in vacuum. For the saturable absorber, the total population density satisfies the equivalence of $n_{so} = n_{gs} + n_{es}$. In terms of the initial transmission of the saturable absorber T_0, the factor $\sigma_{gs} n_{gs} l_s$ can be given by $\sigma_{gs} n_{gs} l_s = \ln(1/T_0)$ assuming there are no excited-state absorption at the initial condition. For analyzing the process of the passively Q-switching more concisely, the dimensionless parameters are introduced as follows: $\tilde{n} = 2\sigma l_g n$, $\tilde{\phi} = 2\sigma l_{cav} \phi$, $\tilde{n}_{gs} = 2\sigma_{gs} l_s n_{gs}$, $\tilde{n}_{gs} = 2\sigma_{es} l_s n_{es}$, $\tilde{n}_{so} = 2\sigma_{gs} l_s n_{so} = \ln(1/T_0^2)$, and $\tilde{t} = t/t_r$. Using the relation of $n_{so} = n_{gs} + n_{es}$, the excited state population of the saturable absorber $\tilde{n}_{es}$ can be replaced with $\tilde{n}_{es} = \beta\left[\ln(1/T_0^2) - \tilde{n}_{gs}\right]$, where $\beta = \sigma_{es}/\sigma_{gs}$. In terms of the dimensionless parameters, the coupled rate equations for the PQS laser are rewritten as

$$\frac{d\tilde{\phi}}{d\tilde{t}} = \left[\tilde{n} - (1-\beta)\tilde{n}_{gs} - \left(\beta \ln\left(\frac{1}{T_0^2}\right) + \ln\left(\frac{1}{R}\right) + L\right)\right]\tilde{\phi}, \tag{4}$$

$$\frac{d\tilde{n}}{d\tilde{t}} = -\tilde{n}\tilde{\phi}, \tag{5}$$

$$\frac{d\tilde{n}_{gs}}{d\tilde{t}} = -\alpha \tilde{n}_{gs}\tilde{\phi}, \tag{6}$$

where $\alpha = \left(A\sigma_{gs}/A_s\sigma\right)$ is a key factor for the PQS performance as seen in later discussion. Dividing Eq. (5) by Eq. (6) and integrating gives

$$\tilde{n}_{gs} = \tilde{n}_{so}\left(\frac{\tilde{n}}{\tilde{n}_i}\right)^{\alpha} = \ln\left(\frac{1}{T_0^2}\right)\left(\frac{\tilde{n}}{\tilde{n}_i}\right)^{\alpha}, \tag{7}$$

where $\tilde{n}_i$ is the initial inversion population of the gain medium. The value of $\tilde{n}_i$ is determined from the condition that the round-trip gain is exactly equal to the round-trip losses just before the absorber starts to bleach. Thus

$$\tilde{n}_i = \ln\left(\frac{1}{T_0^2}\right) + \ln\left(\frac{1}{R}\right) + L, \tag{8}$$

Dividing Eq. (4) by Eq. (5) and substituting Eq. (7) into the result can lead to

$$\frac{d\tilde{\phi}}{d\tilde{n}} = \left[-1 + (1-\beta)\ln\left(\frac{1}{T_0^2}\right)\left(\frac{\tilde{n}^{\alpha-1}}{\tilde{n}_i^{\alpha}}\right) + \frac{\tilde{n}_{th}}{\tilde{n}}\right], \tag{9}$$

where

Optics EXPRESS

$$\tilde{n}_{th} = \beta \ln\left(\frac{1}{T_0^{\,2}}\right) + \ln\left(\frac{1}{R}\right) + L \tag{10}$$

is the critical inversion population at the point of maximum photon density corresponding to $d\tilde{\phi}/d\tilde{n} = 0$ under the limit of rapid Q-switching ($\alpha \to \infty$). From Eq. (9) it can also be confirmed that $d\tilde{\phi}/d\tilde{n} = 0$ at $\tilde{n} = \tilde{n}_i$. Consequently, the criterion for achieving a stable PQS pulse train depends on the value of $d^2\tilde{\phi}/d\tilde{n}^2$. Once $d^2\tilde{\phi}/d\tilde{n}^2 > 0$ at $\tilde{n} = \tilde{n}_i$, the photon density can effectively grow up to form a giant pulse. With some algebra, it can be derived that $d^2\tilde{\phi}/d\tilde{n}^2\,(\tilde{n} = \tilde{n}_i) = \left[(\alpha - 1)(\tilde{n}_i - \tilde{n}_{th}) - \tilde{n}_{th}\right]/\tilde{n}_i^{\,2}$. Therefore, the second threshold criterion which describes that the saturable absorber should bleach first before the gain saturation to develop a giant pulse can be expressed as [18]

$$\alpha > \frac{x}{x-1}, \tag{11}$$

where $x = \tilde{n}_i/\tilde{n}_{th}$ is the ratio between the initial inversion and the critical inversion, representing the relative initial inversion population. According to the criterion, once the initial transmission of absorber, the reflectivity of output coupler, and the gain medium have been chosen, increasing α by controlling the cavity mode size is of great importance to generate a good PQS pulse train.

Integrating $d\tilde{\phi}/d\tilde{n}$ over $\tilde{n}$ from Eq. (9) yields

$$\tilde{\phi}(\tilde{n}) = \left\{(\tilde{n}_i - \tilde{n}) - \frac{(\tilde{n}_i - \tilde{n}_{th})}{\alpha}\left[1 - \left(\frac{\tilde{n}}{\tilde{n}_i}\right)^{\alpha}\right] - \tilde{n}_{th}\ln\left(\frac{\tilde{n}_i}{\tilde{n}}\right)\right\}. \tag{12}$$

The normalized final inversion population can be determined by the condition of $\tilde{\phi}(\tilde{n}_f) = 0$:

$$(\tilde{n}_i - \tilde{n}_f) - \frac{(\tilde{n}_i - \tilde{n}_{th})}{\alpha}\left[1 - \left(\frac{\tilde{n}_f}{\tilde{n}_i}\right)^{\alpha}\right] - \tilde{n}_{th}\ln\left(\frac{\tilde{n}_i}{\tilde{n}_f}\right) = 0\,. \tag{13}$$

Defining $\eta_E = \left(\tilde{n}_i - \tilde{n}_f\right)/\tilde{n}_i$ as the energy-utilization efficiency, Eq. (13) can be expressed as

$$\eta_E - \frac{1}{\alpha}\left(1 - \frac{1}{x}\right)\left[1 - \left(1 - \eta_E\right)^{\alpha}\right] - \frac{1}{x}\ln\left(\frac{1}{1-\eta_E}\right) = 0\,. \tag{14}$$

This transcendental equation of η_E straightforwardly determines the critical characteristics of PQS performance such as the output pulse energy E_{out} and the maximum peak power P_{peak}. In terms of x and η_E, the output pulse energy and the maximum peak power can be easily found to be given by [15]

$$\begin{aligned} E_{out} &= h\nu_l \frac{A}{2\sigma}\ln\left(\frac{1}{R}\right)\int \tilde{\phi}\, d\tilde{t} = h\nu_l \frac{A}{2\sigma}\ln\left(\frac{1}{R}\right)\ln\left(\frac{\tilde{n}_i}{\tilde{n}_f}\right) \\ &= h\nu_l \frac{A}{2\sigma}\ln\left(\frac{1}{R}\right)\ln\left(\frac{1}{1-\eta_E}\right) \end{aligned} \tag{15}$$

and

Optics EXPRESS

$$P_{peak} = \frac{h\nu_l}{t_r}\frac{A}{2\sigma}\ln\left(\frac{1}{R}\right)\tilde{\phi}(\tilde{n}_f) = \frac{h\nu_l}{t_r}\frac{A}{2\sigma}\tilde{n}_{th}\left\{(x-1)\left[1-\frac{1}{\alpha}\left(1-\frac{1}{x^{\alpha}}\right)\right]-\ln(x)\right\}, \tag{16}$$

where $h\nu_l$ is the energy of single lasing photon. Since the pulse energy directly depends on the energy-utilization efficiency, it is greatly useful to find an analytical approximation for the solution of the transcendental equation given by Eq. (14). Based on the numerical fitting, the dependence of the energy-utilization efficiency η_E on the relative initial population density x can be approximately found to be

$$\eta_E(x,\alpha) = 1-\exp\left[-1.55\left(\frac{\alpha^2-1}{\alpha^2}\right)\left(x-\frac{\alpha}{\alpha-1}\right)^{0.85}\right] \tag{17}$$

for $\alpha > x/(x-1)$. As a result, the output pulse energy can now be explicitly expressed as a function of the parameters x and α. It is worth to note that the analytical expression given by Eq. (17) cannot only be used to practically design PQS lasers but also be applied to the actively Q-switched operation under the rapid Q-switching limit ($\alpha \to \infty$) [15]. With E_{out} and P_{peak}, the effective pulse width can be defined as

$$\tau_p = \frac{E_{out}}{P_{peak}} = \frac{t_r}{\tilde{n}_{th}}\frac{\ln\left[1/(1-\eta_E(x,\alpha))\right]}{\left\{(x-1)\left[1-\frac{1}{\alpha}\left(1-\frac{1}{x^{\alpha}}\right)\right]-\ln(x)\right\}} = \tau_c\frac{\ln\left(\frac{1}{R}\right)+L}{\beta\ln\left(\frac{1}{T_0^2}\right)+\ln\left(\frac{1}{R}\right)+L}\frac{\ln\left[1/(1-\eta_E(x,\alpha))\right]}{\left\{(x-1)\left[1-\frac{1}{\alpha}\left(1-\frac{1}{x^{\alpha}}\right)\right]-\ln(x)\right\}}, \tag{18}$$

where $\tau_c = t_r/\left[\ln(1/R)+L\right]$ is the photon lifetime. Note that τ_p/τ_c directly depends on the values of parameters x and α. Another important parameter for the PQS laser is the pulse repetition rate that is closely related to pump period for building up the initial inversion population $\tilde{n}_i$. For a given pump power P_{in}, the inversion population in a pump duration T is given by

$$\tilde{n}(T) = \frac{2\sigma}{A_p}\frac{P_{in}\tau_f}{h\nu_p}\left[1-\exp\left(-T/\tau_f\right)\right], \tag{19}$$

where A_p is the pump mode area, $h\nu_p$ is the energy of the pump photon, and τ_f is upper-level lifetime of gain medium. From Eq. (19) the threshold pump power for generating a PQS pulse can be found to be given by $P_{th} = \left(h\nu_p A_p \tilde{n}_i\right)/\left(2\sigma\tau_f\right)$. Once the given pump power $P_{in} > P_{th}$, the pump period T_r for building up the initial inversion population $\tilde{n}_i$ to generate a PQS pulse can be determined by the following equation:

$$\tilde{n}(T_r) = \tilde{n}_i = \ln\left(\frac{1}{T_0^2}\right)+\ln\left(\frac{1}{R}\right)+L = \frac{2\sigma}{A_p}\frac{P_{in}\tau_f}{h\nu_p}\left[1-\exp\left(-T_r/\tau_f\right)\right], \tag{20}$$

After some algebra, the pulse repetition rate can be found to express as

Optics EXPRESS

$$f_r = \frac{1}{T_r} = \frac{1}{\tau_f \ln\left[\frac{1}{1-(P_{th}/P_{in})}\right]} \xrightarrow{P_{in} \gg P_{th}} \frac{1}{\tau_f}\frac{P_{in}}{P_{th}}. \quad (21)$$

Equation (21) clearly reveals that the pulse repetition rate is proportional to the pump power for a typical PQS laser when $P_{in} \gg P_{th}$. Nevertheless, it is frequently found that there are significant deviations between the calculated results of Eq. (21) and the experiments of diode-pumped PQS lasers especially under a high pump level with a serious thermal lensing effect [11–13].

To include the spatial dependence of the pumping profile and the intracavity photon intensity into the theoretical analysis, we follow the approach proposed in [19] but consider more general forms for the spatial distributions of the pump and lasing modes. Taking the spatial distributions into account, the inversion population densities and the photon density can be expressed as

$$n(x,y,z) = N r_o(x,y,z) \ , \quad (22)$$

$$n_{gs}(x,y,z) = n_{gs} \ , \quad (23)$$

$$\phi(x,y,z) = \Phi \varphi_o(x,y,z) \ , \quad (24)$$

where N is the total number of the inversion population of gain medium, Φ is the cavity photon number, $r_o(x,y,z)$ and $\varphi_o(x,y,z)$ are the normalized densities of the pump and lasing modes. Note that here the ground-state population of absorber is assumed to be uniform at the initial condition [19]. Substituting Eqs. (22)-(24) into Eqs. (1)-(3) then performing the overlapping integrals for the spatial distribution of $r_o(x,y,z)$ and $\varphi_o(x,y,z)$, we obtain spatially dependent coupled rate equations which are in the same form as Eqs. (4)-(6) but with the replacement of $\tilde{\phi} \to \tilde{\Phi}$, $\tilde{n} \to \tilde{N}$, and $\tilde{n}_{gs} \to \tilde{N}_{gs}$. Here the dimensionless parameters with spatial dependence are given by $\tilde{N} = 2\sigma l_g N / V_{eff}$, $\tilde{\Phi} = 2\sigma l_{cav} \Phi / (V_{eff} S)$, and $\tilde{N}_{gs} = 2\sigma_{gs} l_s n_{gs}$, where

$$V_{eff} = \frac{1}{\int r_o(x,y,z)\varphi_o(x,y,z)\,dV} \quad (25)$$

and

$$S = \frac{\left[\int r_o(x,y,z)\varphi_o(x,y,z)\,dV\right]^2}{\int r_o(x,y,z)\varphi_o^2(x,y,z)\,dV} \quad (26)$$

are the effective mode volume and the overlapping efficiency, respectively [24]. Since the coupled rate equations are in the same form as the previous analysis, the approximated solution given by Eq. (17) is still valid to the transcendental equation of $\eta_E = (\tilde{N}_i - \tilde{N}_f)/\tilde{N}_i$ with the spatial dependence, where $\tilde{N}_i = 2\sigma l_g \tilde{n}_i / V_{eff}$ is the initial inversion population and $\tilde{N}_f$ is final inversion population at the end of the PQS process. Consequently, the pulse energy, maximum peak power, effective pulse width, and pulse repetition rate with the consideration of spatially overlapping efficiency can be derived as

Optics EXPRESS

$$\tilde{E}_{out}(x,\alpha) = h\nu_l \frac{SV_{eff}}{2\sigma l_{cav}} \ln\left(\frac{1}{R}\right) \ln\left(\frac{1}{1-\eta_E(x,\alpha)}\right), \tag{27}$$

$$\tilde{P}_{peak} = \frac{h\nu_l}{t_r} \frac{Sl_g}{l_{cav}} \ln\left(\frac{1}{R}\right) \tilde{n}_{th} \left\{(x-1)\left[1-\frac{1}{\alpha}\left(1-\frac{1}{x^a}\right)\right] - \ln(x)\right\}, \tag{28}$$

$$\tilde{\tau}_p = \frac{t_r V_{eff}}{2\sigma l_g} \frac{\ln\left[1/(1-\eta_E(x,\alpha))\right]}{\tilde{n}_{th}\left\{(x-1)\left[1-\frac{1}{\alpha}\left(1-\frac{1}{x^a}\right)\right] - \ln(x)\right\}}, \tag{29}$$

$$\tilde{f}_r = \frac{1}{\tau_f \ln\left[\frac{1}{1-\left(P_{th}V_{eff}/P_{in}A_p l_{cav}\right)}\right]}. \tag{30}$$

It is worth to note that the primary advantage and progress of the present model compared with previous works by other groups [19, 20] are to offer concise expressions that can analytically approximate the performance of pulse repetition rate, pulse energy, pulse width, and peak power under the non-negligible thermal lensing effect for practically designing and analyzing high-power PQS lasers in real applications. In the next section we perform a real case PQS laser system to manifest the modified model with the spatial dependence.

3. Experimental manifestation and discussion

Figure 1 depicts the experimental setup. Considering a typical case for end-pumped PQS lasers with high repetition rate, we choose a 0.2 at. % a-cut Nd:YVO_4 crystal as the gain medium and a Cr^{4+}:YAG crystal as the saturable absorber. The Nd:YVO_4 crystal with the dimensions of 3 × 3 × 12 mm^3 was coated with antireflection (AR) at 808 nm and 1064 nm on both end facets and it was placed at a small distance d_1 to the input mirror for effective pumping. The Cr^{4+}:YAG crystal was also AR coated at 1064 nm on both surfaces and with an initial transmission T_0 = 65% for the lasing wavelength. The laser crystal and the saturable absorber were wrapped with indium foil and mounted in water-cooled copper heat sinks at 16°C. The pump source was a fiber-coupled laser diode at 808 nm with a core diameter of 400 μm and a numerical aperture of 0.14 combined with a reimaging lens set with an effective focal length of 38 mm and a unity magnification. The pump beam was reimaged into the gain crystal with a beam radius $\omega_p \approx 300$ μm considering the beam divergence and with a coupling efficiency of 94%. The input front mirror (FM) was a concave (CV) mirror with the radius of curvature ρ_1 = 100 mm which was coated AR at 808 nm on the entrance face as well as high-transmittance (HT) at 808 nm and HR at 1064 nm at the second facet. For thorough studying the influences of cavity mode on the PQS performance, we choose two output couplers (OCs) with 40% transmission at the lasing wavelength λ_l for comparison: one is a convex (CX) mirror with a radius of curvature ρ_2 = –30 mm while the other is a plane (PL) mirror with $\rho_2 \to \infty$. In order to meet the second threshold criterion for effectively bleaching the absorber, the Cr^{4+}:YAG crystal was placed fairly close to the OC and the cavity length was set to be l_{cav} = 70 mm for tight focusing operation [6].

Optics EXPRESS

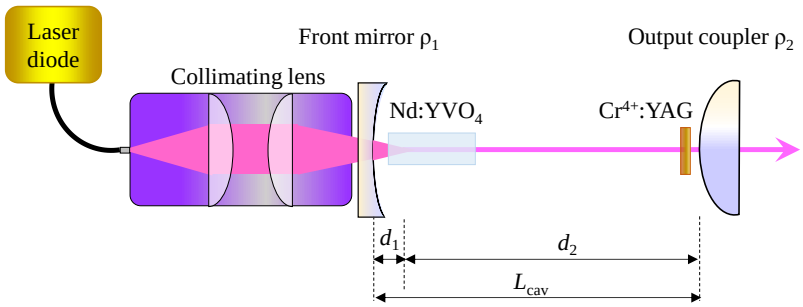

Fig. 1. The experimental setup of a typical end-pumped PQS laser.

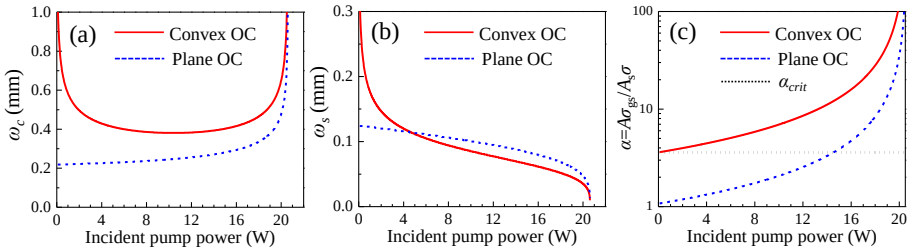

Fig. 2. Effective mode size (a) on the gain crystal ω_c and (b) on the saturable absorber ω_s as functions of the pump power for the cases of CV-CX and CV-PL resonators. (c) The key parameter α as a function of the pump power for the cases of CV-CX and CV-PL resonators. The dotted black line marks the critical value of α for a good PQS performance.

At first we study the variations of cavity mode size for the two configurations of CV-PL and CV-CX resonators under the thermal lensing effect. Utilizing the $\overset{*}{g}$-parameters and the effective cavity length l_{eff} given by

$$g_i^* = 1 - \frac{l_{cav}}{\rho_i} - D d_j \left(1 - \frac{d_i}{\rho_i}\right), \quad i, j = 1,2 \;\&\; i \neq j \;, \tag{31}$$

$$l_{eff} = (d_1 + d_2) - D\, d_1 d_2 \;, \tag{32}$$

the mode size ω_c at the gain medium and the mode size ω_s at the absorber fairly closed to the OC under thermal lensing effect can be respectively written as

$$\omega_c = \sqrt{\frac{\lambda_l l_{eff}}{\pi}} \sqrt{\frac{g_2^*}{g_1^*(1 - g_1^* g_2^*)}} \left[\left(1 - \frac{d_1}{\rho_1}\right)^2 + \left(\frac{d_1}{l_{eff}}\right)^2 \frac{g_1^*(1 - g_1^* g_2^*)}{g_2^*} \right], \tag{33}$$

and

$$\omega_s = \sqrt{\frac{\lambda_l l_{eff}}{\pi}} \sqrt{\frac{g_1^*}{g_2^*(1 - g_1^* g_2^*)}} \;. \tag{34}$$

Here D is the refractive power of thermal lens whose value is proportional to the pump power and inverse proportional to the pump area as $D(P_{in}) = C P_{in} / \omega_p^2$ [25]. Note that $d_1 + d_2 = l_{cav}$ if the thermal lens is considered to be a thin lens. Using $C \approx 2 \times 10^{-5}$ mm/W [25] and substituting the experimental parameters mentioned above into Eqs. (31)-(34), ω_c and ω_s as functions of the pump power can be calculated as shown in Figs. 2(a) and 2(b), respectively. For the case of CV-CX cavity, ω_c first decreases under the cold cavity condition with P_{in} <4 W and

Optics EXPRESS

remains nearly unchanged in the region of P_{in} = 4 W to 16 W and then dramatically rises with the increasing pump power when P_{in} >16 W. On the other hand, the ω_c for the CV-PL cavity keeps growing with the increasing pump power and becomes divergent at about P_{in} = 21 W. The nearly unchanged region of ω_c for the CV-CX cavity implies that the thermal lens can be effectively compensated by choosing a suitable CX mirror as the OC [26, 27]. It can be clearly seen in Fig. 2(a) that the overall cavity mode size of ω_c for the CV-CX cavity is far larger than that of the CV-PL cavity. In other words, the CV-CX resonator can be a more feasible configuration to achieve energy scale-up for PQS lasers [23]. For the mode size on the saturable absorber, it can be found that ω_s decreases with the increasing pump power for both the CV-CX and CV-PL resonators. Nevertheless, the decreasing rate of ω_s with respect to P_{in} for the case of CV-CX cavity is faster than that of CV-PL cavity, which indicates the CV-CX configuration can achieve more effective tight-focusing operation for the PQS lasers. For comparing the two configurations more quantitatively, we analyze the dependence of the key parameter α on the pump power to theoretically examine the PQS performance of the two resonators. Using the results shown in Figs. 2(a) and 2(b) with $\sigma = 2.5 \times 10^{-16}$ mm^2 and $\sigma_{gs} = 8.7 \times 10^{-17}$ mm^2, α as a function of the incident pump power for the CV-CX and CV-PL resonators are calculated as shown in Fig. 2(c). Since Eq. (11) only gives the threshold criterion for PQS operation, here we define the critical value of α_{crit} which satisfies $\eta_E(x, \alpha = \alpha_{crit}) = 0.75\eta_E(x, \alpha \to \infty)$ as a more specific indicator for a good PQS performance. The critical parameter α_{crit} evaluated with x = 1.935 for the present experiment is marked by the black dotted line in Fig. 2(c). It can be clearly seen that for the configuration of CV-CX cavity the critical criterion for good PQS performance is always fulfilled, whereas the α parameter meets the critical value only when P_{in}>15 W in the case of CV-PL cavity. Consequently, it is expected that the stable output pulse trains can only be achieved at higher pump power in the PQS laser with a conventional CV-PL cavity.

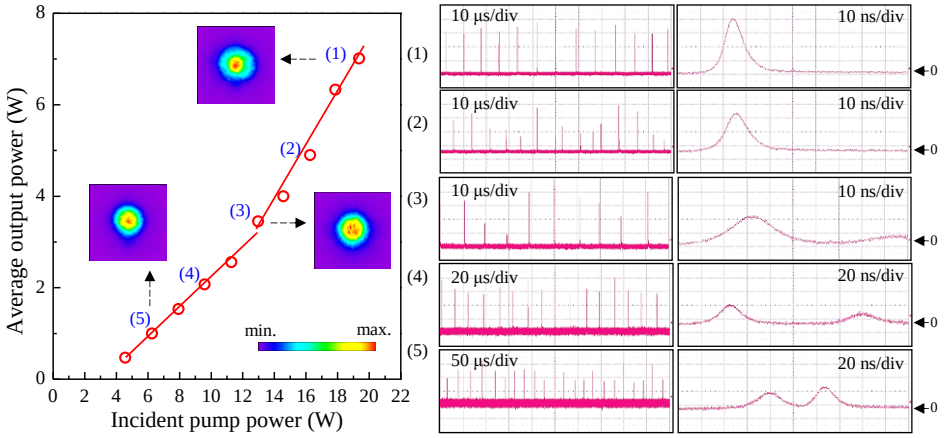

Fig. 3. The experimental results of averaged output power versus incident pump power (left-hand side) and the corresponding PQS pulse trains and single pulse profiles (right-hand side) for the PQS performance of the CV-PL configuration.

Optics EXPRESS

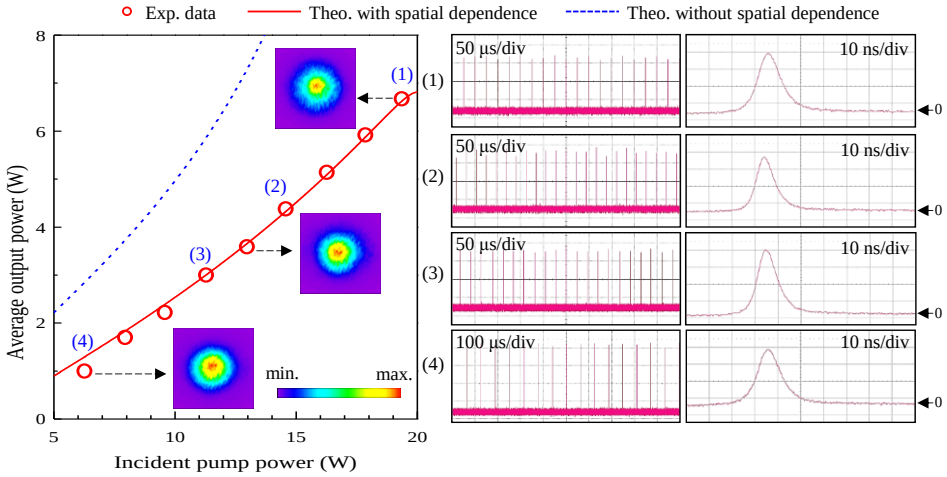

Fig. 4. The experimental results of averaged output power versus incident pump power (left-hand side) and the corresponding PQS pulse trains and single pulse profiles (right-hand side) for the PQS performance of the CV-CX configuration. The solid red line and dashed blue line depict the theoretical predictions by the PQS model with and without the spatial dependence, respectively.

Figure 3 shows the experimental results of averaged output power versus input pump power (left-hand side) and the corresponding PQS pulse trains and single pulse profiles (right-hand side) for the PQS performance of the CV-PL configuration. The output transverse patterns for the PQS laser are also shown in the insets of Fig. 3. The beam quality M^2 factor is estimated to be about 1.25 × 1.31 for the horizontal and vertical directions on the average of each pump power. Since the critical criterion for good PQS operation is only satisfied at higher pump power (P_{in}>15 W) for the case of CV-PL cavity, the dependence of averaged output power on the input pump power is not quiet linear with two segments at lower (P_{in}<15 W) and higher pump power (P_{in}≥15 W) corresponding to two slope efficiencies of 30% and 53%, respectively. On the other hand, it can be clearly seen that the pulse trains at low power show significant amplitude fluctuations with a serious satellite pulse effect originated from the ineffective bleaching of absorber. It is until P_{in}>15 W to meet the critical criterion that the pulse trains become more stable and a single giant pulse can be effectively built up. From the experimental results, the pulse energy, and the peak power at the pump power of 19.4 W with pulse repetition rate of 111 kHz and pulse width of 14 ns are evaluated to be 63.1 μJ and 4.5 kW, respectively.

Figure 4 shows similar plots as Fig. 3 for the PQS performance of the CV-CX configuration. Because the critical criterion for good PQS operation is always satisfied in the CV-CX cavity, it can be found that the dependence of averaged output power on the pump power reveals a fairly linear behavior with an overall slope efficiency up to 46% and an optical-to-optical conversion efficiency of 34.5% at the maximum pump power of 19.6 W. More importantly, the pulse trains composed by the single giant pulses for the PQS laser with the CV-CX resonator show quiet stable behavior with little amplitude fluctuations and timing jitters as seen in Fig. 4. In addition, the M^2 factor for the transverse patterns is estimated to be about 1.27 × 1.24 for the horizontal and vertical directions on the average of each pump power. With the experimental data shown in Fig. 4, the pulse repetition rate, pulse energy, pulse width, and maximum peak power as functions of input pump power are determined and shown in Figs. 5(a)-5(d), respectively. To the best of our knowledge, it is the first-time employment of the concave-convex linear resonator to fulfill a stable PQS laser system with a high repetition rate and a high pulse energy in the end-pumped scheme. Unlike the theoretical prediction from PQS model without spatial dependence given by Eq. (21), it is discovered

Optics EXPRESS

that the pulse repetition rate presents a saturation and decreasing behavior at higher pump power when there is a dominant thermal lensing. As a result, the corresponding pulse energy shows a significant enlargement with the increasing pump power when P_{in}>15 W as seen in Fig. 5(b). The saturation and decrease of repetition rate with increasing pump power mainly comes from the variation of cavity mode size which is closely related to the initial inversion population $\tilde{N}_i = 2\sigma l_g \tilde{n}_i / V_{eff}$ for starting the PQS process. The superior stability of the PQS performance of the CV-CX configuration enables us to manifest the proposed PQS model with spatial dependence carefully. Considering the normalized density distribution of the pump and lasing modes are both Gaussian which can be given by [28]

$$r_o(x,y,z) = \left[\frac{\kappa \exp(-\kappa z)}{1-\exp(-\kappa l_g)}\right]\left(\frac{2}{\pi\omega_p^2}\right)\exp\left[-\frac{2\left(x^2+y^2\right)}{\omega_p^2}\right], \tag{35}$$

and

$$\varphi_o(x,y,z) = \left(\frac{2}{\pi\omega_c^2 l_{cav}}\right)\exp\left[-\frac{2\left(x^2+y^2\right)}{\omega_c^2}\right], \tag{36}$$

where κ is the gain coefficient of the gain medium, the effective mode volume and the overlapping efficiency can be evaluated as

$$V_{eff} = \left[\pi\left(\omega_c^2+\omega_p^2\right)l_{cav}\right]/2, \tag{37}$$

and

$$S = \frac{\omega_c^2\left(\omega_c^2+2\omega_p^2\right)}{\left(\omega_c^2+\omega_p^2\right)^2}. \tag{38}$$

Substituting Eqs. (37) and (38) into Eqs. (27)-(30) with the experimental parameters, the theoretical predictions for the PQS performance by the spatially dependent model are calculated and shown by the red solid lines in Figs. 5(a)-5(d). For comparisons, the theoretical results given by the PQS model without spatial dependence are also calculated and shown by the blue dashed lines in Figs. 5(a)-5(d). Note that we also used the calculated results of pulse repetition rate and pulse energy to analyze the averaged output power with $P_{out} = E_{out} \times f_r$ as shown in Fig. 4. It can be clearly seen that all the experimental results of the PQS performance can be described by the proposed spatially dependent model with excellent consistency. The good agreement between the experimental results and the theoretical analyses not only verifies the validity of the proposed model for describing the performance of high-power PQS lasers with a significant thermal lensing effect but also sheds light on using the theoretical predictions to design high-pulse-energy and high-peak-power lasers with higher accuracy.

Optics EXPRESS

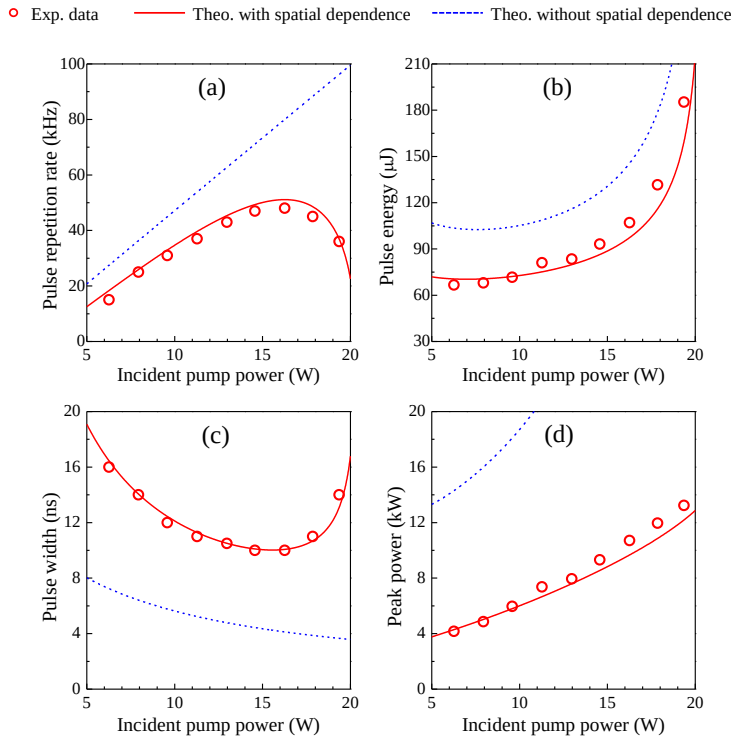

Fig. 5. The (a) pulse repetition rate, (b) pulse energy, (c) pulse width, and (d) maximum peak power as functions of incident pump power analyzed from the results shown in Fig. 4. The solid red line and dashed blue line depict the theoretical predictions by the PQS model with and without the spatial dependence, respectively.

4. Conclusion

In conclusion, a thorough derivation from the coupled rate equations of PQS operation have been reviewed to give a transcendental equation which determines the key properties of PQS lasers. It has been numerically found that the solution of the transcendental equation can be approximated by an analytical function which is not only practical for analyzing PQS laser but also valid for active Q-switched operation. The theoretical treatment has been further generalized into a spatially dependent model which includes the spatial overlapping between the pump and lasing modes under the thermal lensing effect. To verify the modified PQS model with the spatial dependence, an end-pumped Nd:YVO_4/Cr^{4+}:YAG system with a concave-convex resonator has been utilized for manifestation. Compared with the typical configuration of a concave-plano cavity for a PQS laser, the concave-convex resonator has been confirmed to show superior advantage that can easily achieve the critical condition for a good PQS performance to generate fairly stable pulse trains with small amplitude fluctuations and little timing jitters. With the stable output performance from the PQS laser with the concave-convex resonator, we have validated that the proposed spatially dependent model can describe all experimental results in perfect consistency. The good agreement between the experimental results and the theoretical predictions sheds light on using the proposed model to design and analyze the high-power end-pumped PQS lasers under a strong thermal lensing effect with very high accuracy.

Funding

Ministry of Science and Technology of Taiwan (Contract No. MOST-105-2628-M-009-004 and MOST-105-2112-M-009-012).